JOURNAL OF GEOPHYSICAL RESEARCH, VOL. 113, D00A19, doi:10.1029/2008JD009837, 2008

Global Moderate Resolution Imaging Spectroradiometer (MODIS) cloud detection and height evaluation using CALIOP

R. E. Holz,[1] S. A. Ackerman,[1] F. W. Nagle,[1] R. Frey,[1] S. Dutcher,[1] R. E. Kuehn,[2] M. A. Vaughan,[2] and B. Baum[1]

Received 16 January 2008; revised 4 August 2008; accepted 26 August 2008; published 19 December 2008.

[1] A global 2-month comparison is presented between the Cloud-Aerosol Lidar with Orthogonal Polarization (CALIOP) and the Moderate Resolution Imaging Spectroradiometer (MODIS) for both cloud detection and cloud top height (CTH) retrievals. Both CALIOP and MODIS are part of the NASA A-Train constellation of satellites and provide continuous near-coincident measurements that result in over 28 million cloud detection comparisons and over 5 million CTH comparisons for the months of August 2006 and February 2007. To facilitate the comparison, a computationally efficient and accurate collocation methodology is developed. With the collocated MODIS and CALIOP retrievals, nearly instantaneous comparisons are compiled regionally and globally. Globally, it is found that the MODIS 1-km cloud mask and the CALIOP 1-km averaged layer product agreement is 87% for cloudy conditions for both August 2006 and February 2007. For clear-sky conditions the agreement is 85% (86%) for August (February). The best agreement is found for nonpolar daytime and the poorest agreement in the polar regions. Differences in cloud top heights depend strongly on cloud type. Globally, MODIS underestimates the CTH relative to CALIOP by 1.4 ± 2.9 km for both August 2006 and February 2007. This value of 1.4 km is obtained using the CALIOP 1 km layer products. When compared to the CALIOP 5-km products, the differences increase to −2.6 ± 3.9 km as a result of CALIOP's increased sensitivity to optically thin cirrus. When only high clouds above 5 km are considered, the differences are found to be greater than 4 km with individual comparisons having differences larger than 10 km. These large differences (>10 km) represent approximately 16% of the nonpolar high cloud retrievals (>5 km). For high clouds it is found that MODIS retrieves a cloud top height for 90% of the clouds detected by the CALIOP 5-km layer products. The large MODIS underestimates for optically thin cirrus occur for cases when MODIS reverts to a window brightness temperature retrieval instead of CO_2 slicing. A systematic bias is found for marine low-level stratus clouds, with MODIS overestimating the CTH by over 1 km in dense marine stratocumulus regions. The cause of the bias was identified in the MODIS Collection 5 algorithm; an application of a modified algorithm reduced this bias.

Citation: Holz, R. E., S. A. Ackerman, F. W. Nagle, R. Frey, S. Dutcher, R. E. Kuehn, M. A. Vaughan, and B. Baum (2008), Global Moderate Resolution Imaging Spectroradiometer (MODIS) cloud detection and height evaluation using CALIOP, *J. Geophys. Res.*, *113*, D00A19, doi:10.1029/2008JD009837.

1. Introduction

[2] Understanding the impact of clouds on the Earth's radiation balance and detecting changes in the amount and distribution of global cloud cover requires an accurate global cloud climatology with well-characterized uncertainties. To meet this challenge, significant effort has been given to generating climate quality long-term cloud data sets using over 30 years of polar-orbiting infrared satellite measurements [*Ackerman et al.*, 1998; *Heidinger*, 2003; *Rossow and Schiffer*, 1999; *Wylie and Menzel*, 1999] with plans to continue the cloud record using the next generation of polar orbiting sensors. A "Climate Quality" climatology requires that both the uncertainties and the physical sensitivities are quantified and are smaller than the expected climate signature. Uncertainties resulting from the fundamental measurement (instrument noise, radiometric bias) can be determined analytically as part of the retrieval process [*Heidinger*, 2003]. However, these uncertainties account for only part of the total error budget. The more difficult uncertainties result from physical approximations used to develop the retrieval methodology. Additionally, further uncertainties

[1]Cooperative Institute for Meteorological Satellite Studies, University of Wisconsin-Madison, Madison, Wisconsin, USA.
[2]Science Systems and Applications, Inc., Hampton, Virginia, USA.

0148-0227/08/2008JD009837$09.00

may be introduced by the ancillary data sets used in the retrieval process, such as land emissivity and atmospheric profiles of temperature, water vapor, and ozone. The difficulty in characterizing these uncertainties is compounded by their strong regional dependence. For example, an infrared (IR) cloud height retrieval algorithm may work very well near the equator, yet be very uncertain over the polar regions owing to the lack of thermal contrast between the clouds and the surface. Assessing these uncertainties requires comparisons with sets of well-characterized measurements having global extent. This study provides such an assessment using global lidar measurements provided by the Cloud-Aerosol Lidar with Orthogonal Polarization (CALIOP).

[3] Significant effort has been given to characterizing the uncertainties and sensitivities of various global cloud climatologies using independent evaluation measurements from ground, aircraft, and more recently satellite platforms [*Ackerman et al.*, 2008; *Holz et al.*, 2006; *Kahn et al.*, 2007a; *Mahesh et al.*, 2004; *Min et al.*, 2004; *Thomas et al.*, 2002; *Zhao and Girolamo*, 2006]. These comparisons have provided important insight but have been limited by the relatively small number of comparisons and the lack of global coverage. Recent advances in active remote sensing technology have provided satellite-based lidar and radar measurements. For example, the Geosciences Laser Altimeter System (GLAS) was launched on the Ice, Cloud and Land Elevation Satellite (ICESat) platform in January 2003, and provided the first satellite-based atmospheric lidar measurements [*Abshire et al.*, 2005]. The GLAS measurements provided a valuable resource for evaluating cloud retrievals [*Ackerman et al.*, 2008; *Mahesh et al.*, 2004; *Wylie et al.*, 2007]. In a comparison of GLAS to HIRS, the HIRS global cloud frequency was 5% greater than GLAS and HIRS underestimated CTH with differences larger than 4 km in the tropics. The comparison was done statistically because of the infrequent intersections of GLAS with the sun synchronous NOAA polar-orbiting satellites carrying HIRS.

[4] The successful launch of the CALIOP onboard NASA's Cloud Aerosol Lidar and Infrared Pathfinder Satellite Observation (CALIPSO) satellite provides vertically resolved measurements of both cloud and aerosols with near coincident sampling to MODIS on the Aqua satellite. This new data set provides a new opportunity to evaluate the passive retrievals. A recent 5-day evaluation of the Atmospheric Infrared Sounder (AIRS) cloud retrievals using CALIOP found significant biases in the cloud height determination compared to CALIOP for thin cirrus but with smaller biases for low clouds [*Kahn et al.*, 2007b]. When accurately collocated with MODIS, CALIOP provides a global evaluation data set that can be compared directly to the MODIS passive cloud retrievals. The resulting evaluation of the MODIS cloud mask and cloud top height (CTH) retrievals are presented in this paper.

[5] This paper is organized as follows. A description of the MODIS and CALIOP cloud retrievals is provided in section 2 including a discussion of the MODIS/CALIOP collocation algorithm developed for the comparison. The results of 2 months (August 2006 and February 2007) of global collocated CALIOP and MODIS comparisons of cloud detection and cloud top height are presented in section 3, followed by a detailed discussion of the results. Conclusions are then presented in section 4.

2. Measurements and Collocation

[6] The NASA Earth Observing System (EOS) A-Train [*Stephens et al.*, 2002] is a series of satellites flying in close formation carrying passive and active sensors that provide a diverse suite of coincident measurements that characterize the three-dimensional structure of the Earth's atmosphere. This paper focuses on comparing the active sensor cloud profiles provided by CALIOP onboard CALIPSO with the passive sensor cloud products from MODIS on the Aqua platform. There are significant differences in the spatial sampling between MODIS and CALIOP that are discussed later in this section. Furthermore, there are also temporal sampling differences as the CALIPSO orbit trails MODIS on Aqua by approximately 80 s. To minimize the uncertainties resulting from the spatial and temporal sampling differences, a collocation methodology has been developed and as outlined in Appendix A. Accurate collocation provides the ability to perform direct comparisons between CALIOP and MODIS ground-projected instantaneous field-of-view (GIFOV) measurements. Descriptions of the MODIS and CALIOP instruments, and of their respective Level-2 cloud retrieval algorithms, are now presented.

2.1. MODIS

[7] MODIS (Moderate Resolution Imaging Spectroradiometer) measures radiances at 36 wavelengths, including infrared and visible bands with spatial resolution 250 m to 1 km. The cloud mask is part of the MODIS Cloud Product Suite and is described by *Ackerman et al.* [2008, 1998], *Frey et al.* [2008], *King et al.* [2003], and *Platnick et al.* [2003].

[8] The MODIS cloud mask algorithm uses a series of sequential tests on the passive reflected solar and infrared observations to indicate a level of confidence that MODIS is observing a clear-sky scene. Produced for the entire globe, day and night, and at 1-km resolution, the cloud mask algorithm employs up to nineteen MODIS spectral bands to maximize reliable cloud detection. In addition, a 250-m mask is derived from the two 250 m resolution bands (0.65 and 0.86 μm).

[9] As cloud cover can occupy less than the full pixel (i.e., subpixel clouds), the MODIS cloud mask is designed for varying degrees of clear sky confidence; that is, it provides more information than a simple yes/no decision. The cloud mask consists of 48 bits of output per pixel and includes information on individual cloud test results, the processing path, and ancillary information (e.g., land/sea tag). The first two bits of the mask summarize the results from all individual tests by classifying cloud contamination in every pixel of data as either confident clear, probably clear, uncertain/probably cloudy, or cloudy.

[10] The MODIS cloud mask algorithm identifies several conceptual domains according to surface type and solar illumination including land, water, snow/ice, desert, and coast for both day and night. Once a pixel is assigned to a particular domain, thereby defining an algorithm path, a series of threshold tests attempts to detect the presence of clouds or optically thick aerosol in the instruments FOV. Each test returns a confidence level that the pixel is clear, ranging in value from 1 (high confidence clear) to 0 (low

Table 1. CALIOP Instrument Characteristics

Characteristic	Value
Laser wavelengths	532,1064 nm
Rep rate	20.16 Hz
Pulse length	20 nsec
Beam divergence	100 urad
Telescope IFOV	130 μrad
Surface GIFOV diameter	70 m

confidence clear). There are several types of threshold tests used to detect various cloud conditions. Those capable of detecting similar cloud conditions are grouped together. It should be noted that few, if any, spectral tests are completely independent. *Ackerman et al.* [2008] compared the MODIS cloud mask with various ground based and aircraft based active systems and found agreement approximately 85% of the time. Through comparison with high-spectral resolution lidar, *Ackerman et al.* [2008] found that over land the optical depth detection limit of MODIS is approximately 0.3 to 0.4.

[11] Cloud top pressure (CTP) is derived using 5 thermal infrared bands (both day and night) at 5 km spatial resolution by applying the CO_2 slicing technique as discussed in detail by *Menzel et al.* [2008]. The CO_2 slicing technique is used to infer CTP and effective cloud amount for opaque and nonopaque midlevel to high-level single layer clouds. Retrievals are derived from ratios of differences in radiances between cloudy and clear-sky regions at two nearby wavelengths. In MODIS operational processing, CTP is calculated for the following ratio pairs: 14.2 μm/13.9 μm; 13.9 μm/13.6 μm, 13.6 μm/13.3 μm, and 13.9 μm/13.3 μm. The cloud emissivity is assumed to be identical in the spectral band pairs. The optimal CTP is selected that best satisfies the forward radiative transfer calculations [*Menzel et al.*, 2008]. The fundamental CO_2 slicing retrievals are pressure and effective emissivity (defined as cloud emissivity multiplied by cloud fraction) applied to a 5×5 pixel array, for a product at a nominal resolution of 5 km^2 where at least 4 of the 25 pixels must be flagged as probably cloudy or cloudy by the cloud mask. The algorithm uses analyses from the Global Data Assimilation System (GDAS) meteorological profile product (1° spatial and 6 h temporal resolution), and the National Center for Environmental Prediction (NCEP) Reynolds Blended Sea Surface Temperature (SST) product to calculate the required clear-sky radiances. Once the CTP is determined for a given 5 km^2 FOV, a cloud top height (CTH) and cloud temperature is determined using the NCEP Global Forecast System (GFS). Differences between model-derived and measured clear-sky radiances are mitigated with a radiance bias adjustment to avoid height assignment errors [*Menzel et al.*, 2008].

[12] Error analyses in CTP/CTH retrievals from the CO_2 slicing method have been investigated in several studies [*Hawkinson et al.*, 2005; *Holz et al.*, 2006; *Naud et al.*, 2004; *Smith and Platt*, 1978; *Wielicki and Coakley*, 1981]. Cloud height accuracy increases as the observed cloud signal (the clear sky minus the measured radiance) increases for a FOV. For clouds at pressures greater than 700 hPa (i.e., close to the surface), the signal-to-noise ratio decreases, thereby precluding application of the method. For multilayer clouds, CO_2 slicing produces a CTP for the radiative mean of the two clouds, thus misrepresenting the height of both. For low-level clouds, the 11-μm infrared window brightness temperature is used to determine a cloud top temperature assuming the cloud is opaque, and a cloud top pressure is assigned by comparing the measured brightness temperature to that calculated using a simple radiative transfer model using NCEP (GDAS) temperature and humidity profiles. To date, comparisons of the CO_2 slicing method with active sensors have been limited in scope, either to a field campaign or a limited geographic region.

2.2. CALIOP

[13] The Cloud-Aerosol Lidar with Orthogonal Polarization (CALIOP) instrument aboard CALIPSO uses a diode-pumped Nd:YAG laser transmitting at wavelengths of 1064 and 532 nm. In addition to range-resolved measurements of backscatter intensity at each of the two wavelengths, CALIOP also measures linear depolarization ratios at 532 nm, using polarization sensitive optics in the receiver to separate the backscattered radiation into components perpendicular and parallel to the polarization vector of the linearly polarized output of the laser transmitter [*Winker et al.*, 2004, 2007]. CALIOP provides nadir only measurements. Table 1 presents the instrument transmitter and receiver characteristics.

[14] A significant amount of preprocessing is conducted onboard CALIOP before the data is downlinked to the receiving stations. This includes vertical and spatial averaging of the raw lidar profiles, with the amount of averaging a function of altitude above mean sea level. At the maximum resolution, the CALIOP surface footprint has a horizontal spacing of ~333 m with a vertical resolution of 30 m. This resolution is only available for those portions of the profiles lower than 8.2 km. Above 8.2 km the vertical and horizontal averaging varies according to the specifications presented in Table 2. The raw data received from CALIOP are geolocated and calibrated, so that Level 1 profiles of attenuated backscatter coefficients can be generated [*Reagan et al.*, 2002]. The Level-2 cloud products are then derived directly from the Level 1 profile products. To identify layer boundaries, a feature finder is used to separate legitimate features of interest from the noise and calibration uncertainties associated with the Level 1 attenuated backscatter profiles [*Vaughan et al.*, 2004]. Just as the MODIS cloud mask uses detection thresholds, the sensitivity and accuracy of the CALIOP feature finder is dependent on the amount of averaging applied and the threshold levels used to differentiate between noise excursions and genuine atmospheric features. Unlike passive measurements, the active CALIOP measurements resolve the vertical profile with a signal intensity measured at each range interval, allowing for accurate vertical detection sensitivity. The ability for the Level-2 feature finder to detect a feature is thus additionally dependent on both the feature's backscatter intensity and the magnitude of the background signal. The signal at the receiver is a function of the intensity of the backscatter and the attenuation of the atmosphere between the layer of interest and the instrument. For this reason, the sensitivity of the feature finder is not a constant. Fortunately, for this comparison the primary interest is the first layer detected by CALIOP. For this layer, the only attenuation is from molecules and ozone, and the influence of each is small at 532 nm.

[15] The total intensity of the background signal measured by the lidar is dependent on the detector noise,

Table 2. CALIOP Vertical and Horizontal Averaging

Altitude (km)	Horizontal Resolution (km)	Vertical Resolution (m)
31.1–40	5.0	300
20.2–30.1	1.67	180
8.2–20.2	1.0	60
−0.5–8.2	0.33	30

receiver instantaneous field-of-view (IFOV) and width of the spectral filter used to reduce solar background energy scattered into the receiver. For daylight operations the solar background signal dominates the total background signal, decreasing the CALIOP sensitivity to optically thin clouds.

[16] Once a feature is detected, the type is determined using multidimensional probability functions to distinguish clouds from aerosol layers [*Liu et al.*, 2004]. This determination is made using the layer center altitude, the layer mean 532 nm attenuated backscatter and the ratio between the 532 nm and 1064 nm channels (color ratio). A confidence function based on these two measurements is used to determine the probability of the layer containing aerosols or cloud. Once the determination has been made, the layer properties are recorded in separate output files. For this investigation, only the cloud property files are used. As will be discussed, uncertainties in the CALIOP determination of cloud versus aerosol can impact the MODIS evaluation.

[17] Averaging the CALIOP measurements increases the signal to noise, thus increasing the feature finder's sensitivity to optically thin aerosol and cloud layers, but at the cost of reduced spatial and vertical resolution. CALIOP employs a nested, multigrid averaging and detection scheme that searches for layers at horizontal resolutions of 5 km, 20 km, and 80 km. The layers detected during these successive searches are all reported in the 5-km layer products. If a layer is detected within a profile averaged to a 5-km horizontal resolution, the data in that region are subsequently analyzed at progressively finer resolutions of 1 km and 333 m. Layers detected at these higher spatial resolutions are recorded in the 1-km and 333-m cloud layer files. If the backscatter return is too weak to be detected by the 1-km or 333-m averages, the cloud layer will only be reported in the lower resolution files. At the highest resolution, approximately 3–4 CALIPSO profiles will fall within a single MODIS 1-km pixel. At the 5-km resolution, the CALIOP data are undersampled relative to the MODIS 1-km pixel, presenting an interesting problem for comparing the measurements. Using the 5-km cloud boundary file maximizes the CALIOP sensitivity to thin cirrus, but can lead to increased uncertainty because of the sampling differences if the cloud features are smaller than the CALIOP 5-km sampling. To correctly represent the full layer profile information in the 5-km layer products it is necessary to merge the 1-km and 5-km layer products since the 5-km layer products do not always contain all layers detected by CALIOP. The layer products are merged into a new 5 km mask filled using both the CALIOP 5 km and 1-km products. New 5-km cloud boundaries were then generated from this mask. In contrast, the high spatial resolution 333-m data, which have reduced cloud sensitivity and are only available below 8.2 km, oversamples the 1-km MODIS pixel, enabling investigation of subpixel cloud features. The CALIOP retrieval products used in the comparison was version V1–10.

2.3. Collocation and Evaluation Methodology

[18] To avoid sampling regions of the MODIS swath affected by sun glint, the CALIPSO orbit has a slightly different inclination relative to Aqua, resulting in CALIPSO slowly precessing across the MODIS swath crossing the Aqua nadir position near the poles. Comparisons require that both the MODIS pixel transected by CALIOP be identified along with the associated CALIOP shots within the selected MODIS pixel. An accurate and computationally efficient collocation process has been developed to facilitate global comparisons of the MODIS and CALIOP cloud retrievals (see Appendix A). Figure 1 presents a graphical representation of the different combination of the MODIS and CALIOP spatial resolutions: a MODIS 250-m resolution broken cloud image is layered under simulated MODIS 1-km and 5-km footprints to illustrate the importance of accounting for spatial sampling differences between CALIOP and MODIS.

[19] In this study there are three combinations of CALIOP and MODIS spatial resolutions. For MODIS, the cloud mask is generated at 1-km resolution while the cloud top heights are retrieved using a 5 × 5 group of 1-km pixels. For CALIOP, the cloud layer products are available at 333-m, 1-km, 5-km, 20-km, and 80-km horizontal resolutions. Figure 1b presents the collocation geometry for the MODIS 1-km cloud mask and the CALIOP 330-m and 1-km retrievals. In this configuration the MODIS 1-km GIFOV is the "reference" with multiple CALIOP measurements

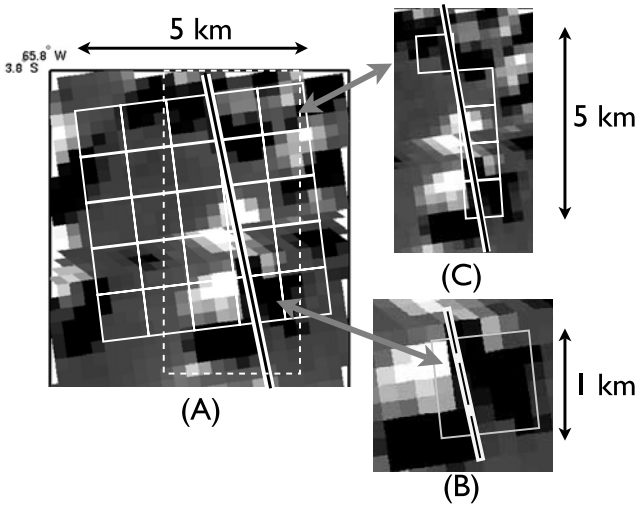

Figure 1. MODIS 0.855 μm MODIS image is overlaid with the three collocation geometries. The surface footprint of CALIOP is presented as the white and black line. (a) The 5-km MODIS footprint (large single box) with the MODIS 1-km footprint geometry (small boxes). (b) The 1-km MODIS GIFOV collocated with the 330-m CALIOP measurements. There are approximately 3 CALIOP shots within the 1-km footprint. (c) Collocation geometry for the 5 km CALIOP averaged retrieval collocated with the 1-km MODIS data. For case C, there are multiple MODIS GIFOV for each CALIOP retrieval.

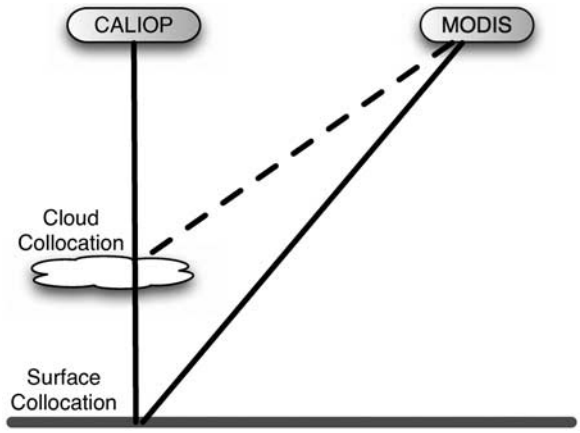

Figure 2. Geometry of the cloud height dependence on the MODIS/CALIOP collocation is presented. The dashed line represents the MODIS cloud collocated scan position while the solid line is the ground collocation.

within the MODIS GIFOV. The CALIOP beam width is approximately 90 m and does not sample the entire MODIS 1 km GIFOV. The collocation of the CALIOP 5 km averaged cloud products is presented in Figure 1c. For this case, multiple MODIS 1-km GIFOV are collocated with the single 5-km CALIOP averaged retrieval which now serves as the reference. In this configuration multiple MODIS GIFOVs are collocated for a single CALIOP retrieval.

[20] The collocation geometry for the MODIS cloud top height comparison with CALIOP is presented in Figure 1a. The collocation geometry is similar to that in Figure 1b but now the MODIS footprint is 5 × 5 km. For the CALIOP full resolution 330-m retrievals, up to 16 CALIOP cloud heights can fall within a single MODIS 5-km FOV. Because the width of the CALIOP footprint does not change with averaging, the sampling percentage of the MODIS 5-km scenes sampled by CALIOP is significantly smaller than the samples within the MODIS 1-km GIFOV. Uncertainties in the comparison resulting from the spatial mismatch need to be considered when interpreting the cloud top height comparisons.

[21] Because CALIOP does not follow the nadir flight track of Aqua, there is a parallax effect resulting in a CTH dependence on the collocation as illustrated in Figure 2. The CTH dependence on the collocation can result in a shift/offset of more than 5 pixels compared to the surface collocation. The collocation algorithm accounts for this offset using the CALIOP CTH. The parallax corrected collocation is presented in this paper.

3. Results

[22] Two months (August 2006 and February 2007) of global collocated MODIS and CALIOP cloud detection and CTH retrievals were compared. The 2 months of collocated MODIS/CALIOP comparisons results in approximately 28 million GIFOV; the 5 km CTH retrievals include over 5 million cases. The selection of a month each in summer and winter allows for the investigation of seasonal changes on the MODIS cloud mask and height detection. The results have been separated by month and include global and regional statistics of the agreement with CALIOP.

3.1. Cloud Mask

[23] The MODIS 1-km cloud mask was evaluated using the collocated CALIOP Level-2 1-km, and 5-km cloud layer retrievals. The MODIS cloud mask results are compared with CALIOP and the results presented as a fractional agreement between the two systems. At the extremes, there are two cases: (1) if the MODIS cloud mask agrees perfectly with CALIOP, the fractional agreement will be one, while (2) no agreement results in a fraction of zero.

[24] The global results of the cloud mask comparison for both the 1-km and 5-km CALIOP cloud products for August 2006 and February 2007 are presented in Table 3. For the comparison, a MODIS cloud mask result is considered cloudy if the cloud mask returns confident cloud or probably cloudy, while a MODIS pixel is defined clear if the MODIS cloud mask returns probably clear or confidently clear. Only MODIS pixels where all the collocated CALIOP retrievals are identical (i.e., either all clear or all cloudy) are included in the statistics in Table 3. As a result of this requirement, approximately 7% of the collocated scenes are not included in the statistics.

[25] The results for August 2006 and February 2007 are separated by clear and cloudy FOVs as determined by CALIOP in columns 2–4 of Table 3. Comparisons of MODIS with both 1-km and 5-km (shown in parentheses)

Table 3. Fractional Agreement That a Clear/Cloudy Scene was Consistently Identified by Both MODIS and CALIOP Instruments, During the Periods August 2006 and February 2007[a]

	August 2006 Clear	August 2006 Cloudy	February 2007 Clear	February 2007 Cloudy
Global CALIOP 1 km (5 km)	0.85 (0.75)	0.87 (0.85)	0.86 (0.77)	0.87 (0.84)
Nonpolar ocean CALIOP 1 km (5 km)	0.87 (0.83)	0.92 (0.86)	0.88 (0.79)	0.92 (0.86)
Nonpolar land CALIOP 1 km (5 km)	0.90 (0.86)	0.85 (0.78)	0.82 (0.74)	0.85 (0.81)
Northern midlatitude CALIOP 1 km (5 km)	0.89 (0.82)	0.88 (0.85)	0.78 (0.68)	0.91 (0.89)
Tropics CALIOP 1 km (5 km)	0.88 (0.84)	0.90 (0.83)	0.89 (0.86)	0.87 (0.80)
Southern midlatitude CALIOP 1 km (5 km)	0.87 (0.81)	0.94(0.92)	0.88 (0.81)	0.93 (0.90)
Arctic > 60° latitude	0.74 (0.62)	0.91 (0.92)	0.83 (0.66)	0.72 (0.76)
Antarctic < −60° latitude	0.79 (0.57)	0.71 (0.75)	0.92 (0.87)	0.88 (0.86)
Northern midlatitude day/night CALIOP 1 km	0.91/0.87	0.88/0.88	0.77/0.80	0.92/0.89
Tropics day/night CALIOP 1 km	0.89/0.86	0.89/0.90	0.90/0.86	0.86/0.87
Southern midlatitude day/night CALIOP 1-km	0.91/0.84	0.93/0.94	0.91/0.86	0.93/0.94

[a]Columns 2–5 show the comparison results for clear and cloudy scenes as determined CALIOP. The first eight rows show the impact of CALIOP averaging over 1 km, and the 5-km averaging in parentheses. The bottom three rows show the results of regional day and night comparisons.

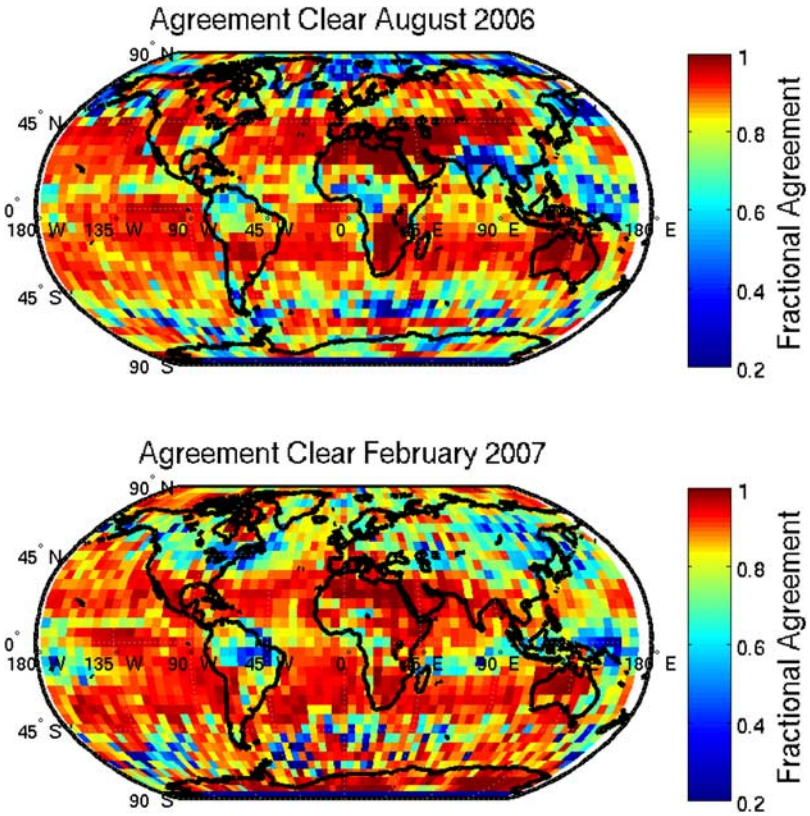

Figure 3. Fractional agreement between the MODIS 1-km and CALIOP 1-km cloud mask for clear scenes is presented. The fractional agreement is calculated here at 5-degree resolution. A grid cell with perfect MODIS agreement will have a fractional agreement of 1 (red), while regions of poorer agreement are colored blue.

CALIOP averaged cloud products are shown in rows 1–8, categorized by region. Rows 9–11 categorize the comparisons by day and night for the 1-km CALIOP and MODIS products.

[26] The global agreement between MODIS and CALIOP 1-km layer products in identifying clear scenes is greater than 85%, which is in general agreement with previous results [*Ackerman et al.*, 2008]. The agreement between both instruments in labeling a nonpolar ocean scene as cloudy is approximately 92% for either month. The best agreement for nonpolar land occurs in August at 90%, and drops to 85% for February. In August, warmer land surfaces and the reduced amount of surface snow/ice in the northern hemisphere both contribute to the increased contrast between clear and cloudy scenes, resulting in an improved clear scene classification. Compared to land, ocean surfaces exhibit less variation in temperature and albedo, and so the agreement over nonpolar oceans is similar for both months.

[27] In general, the MODIS cloud mask compares more favorably with the CALIOP 1-km averaging cloudy scenes than for clear scenes. This result is expected as the MODIS cloud mask was designed to be clear-sky conservative; that is, if there is uncertainty in the spectral tests, the MODIS cloud mask tends to label the scene as cloudy. The exception is the Arctic in February and the Antarctic in both months. In the Arctic region, CALIOP and MODIS agree that the scene is clear 74% of the time in August and 83% of the time in February; they agree that the scene is cloudy 91% of the time in August and only 72% in February. This suggests that during the summer months the MODIS cloud mask applied to the Arctic is biased cloudy while in the winter it is biased clear. [*Ackerman et al.*, 2008] also found better agreement in daylight conditions in the Arctic when comparing MODIS cloud detection to GLAS lidar on ICESAT. For the Antarctic the clear sky agreement is 79% for August and 92% for February; for cloudy scenes the agreement is 71% in August and 88% in February. Detection of a target requires a good contrast between the targets (clouds) and the background (surface). The difficulty of cold background scenes on the algorithm confidence to assign the pixel as clear is also seen in a comparison of the Northern midlatitude region, where the agreement in clear scenes is generally better in the summer month. The cold background scenes of the polar regions make cloud and clear scene discrimination problematic, particularly in the wintertime when only IR channels are available.

[28] Surprisingly, there is little difference in the results when separated by day and night. The agreement in cloud detection is generally within 0.03 for the day and night detection of each region.

[29] A similar comparison was conducted with the CALIOP 5-km layer products using the collocation geometry described in Figure 1c. When the comparisons are made between the MODIS and the CALIOP at 5-km resolution, the clear-sky agreement generally decreases, by 0.05 or

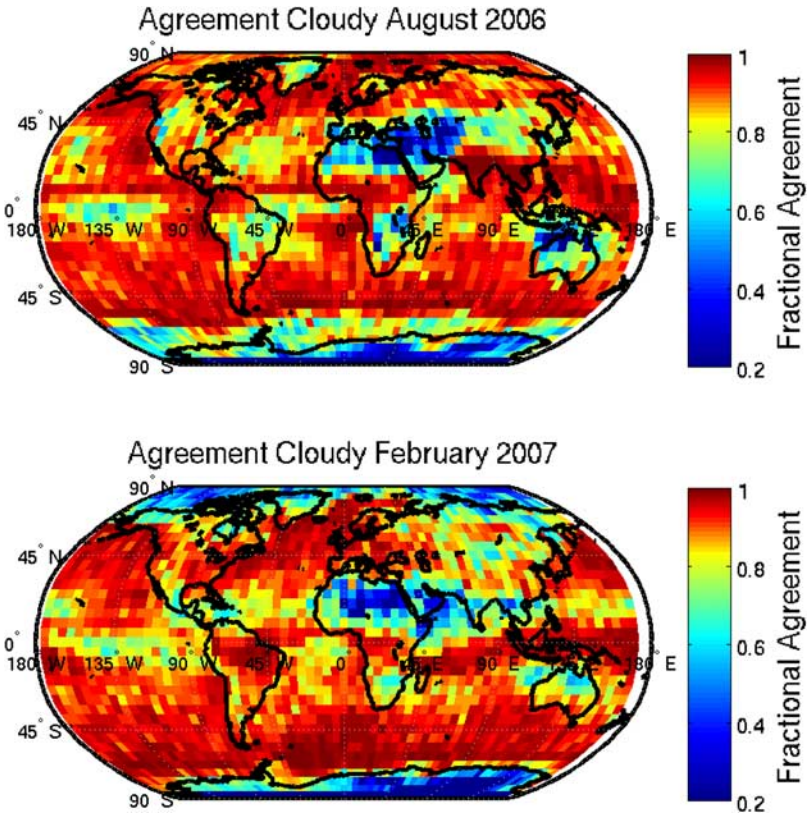

Figure 4. Fractional agreement between the MODIS 1-km and CALIOP 1-km cloud mask for cloudy scenes is presented. The fractional agreement is calculated here at 5-degree resolution. A grid cell with perfect MODIS agreement will have a fractional agreement of 1 (red), while regions of poorer agreement are colored blue.

more, in comparison to the 1-km resolution comparison. When the CALIOP algorithm makes use of an averaging over a 5-km swath, the detection method becomes more sensitive to thin cloud. Since the optical depth limit of cloud detection of MODIS is approximately 0.3–0.4 [*Ackerman et al.*, 2008], optically thin clouds flagged by CALIOP are likely to be labeled clear by MODIS, thereby decreasing the amount of agreement in scene identification. At the larger scale, CALIOP can detect high thin clouds, such as stratospheric clouds, and flag a previously clear scene in the 1-km product as cloudy. This is further discussed below. The increased sensitivity of CALIOP 5-km retrievals to thin cirrus will in general lower the agreement in cloudy scenes as MODIS will continue to label the scene as clear. The increased sensitivity of the CALIOP 5-km product causes the agreement with MODIS to decrease by a few percent for cloudy FOV when compared to the 1-km comparison as presented in Table 3.

[30] The MODIS cloud mask retrieval requires contrast between clear-sky and cloudy-sky conditions that are dependent on both surface and atmospheric properties, and can have significant regional variation. To investigate the regional performance of the cloud mask, the collocated data was divided into five-degree grid cells with the results presented in Figures 3 and 4. While CALIOP and MODIS are in good agreement (i.e., better than 90%) over much of the world, there are regional variations. To help interpret these differences, Figure 5 shows the average cloud height determined from CALIOP for the month of August 2006 for those cases where CALIOP 5-km algorithm detected a cloud and MODIS flagged the scene as clear.

[31] As shown in Figure 3 for clear-sky conditions, MODIS shows disagreement with CALIOP immediately north of the coast of Antarctica. MODIS requires a snow/ice mask in its selection of thresholds. Incorrect scene identification leads to cloud detection errors, which likely contributes to the disagreement around the coast of Antarctica. In February, the disagreement in the midlatitude regions around Russia is associated with cold surfaces, causing misclassification by MODIS. In August, there is also a large difference over the Indian subcontinent that occurs during the summer monsoon season when there are few clear pixels; only a few hundred within a grid box instead of several thousands as in other grid boxes. Disagreement in clear classification also occurs in the periphery of high clouds, the Amazon and the maritime convection region near Indonesia.

[32] In general there is very good agreement in the regional classification of a cloudy scene (Figure 4). The largest differences occur over the polar regions during the winter when the MODIS retrievals rely on thermal methods over cold surfaces. Disagreement occurs over the Antarctica highlands (Figure 4), and Figure 5 indicates that the average height of these clouds missed by MODIS is greater than 12 km, and thus likely optically thin polar stratospheric clouds detected by CALIOP. Disagreement in cloud detec-

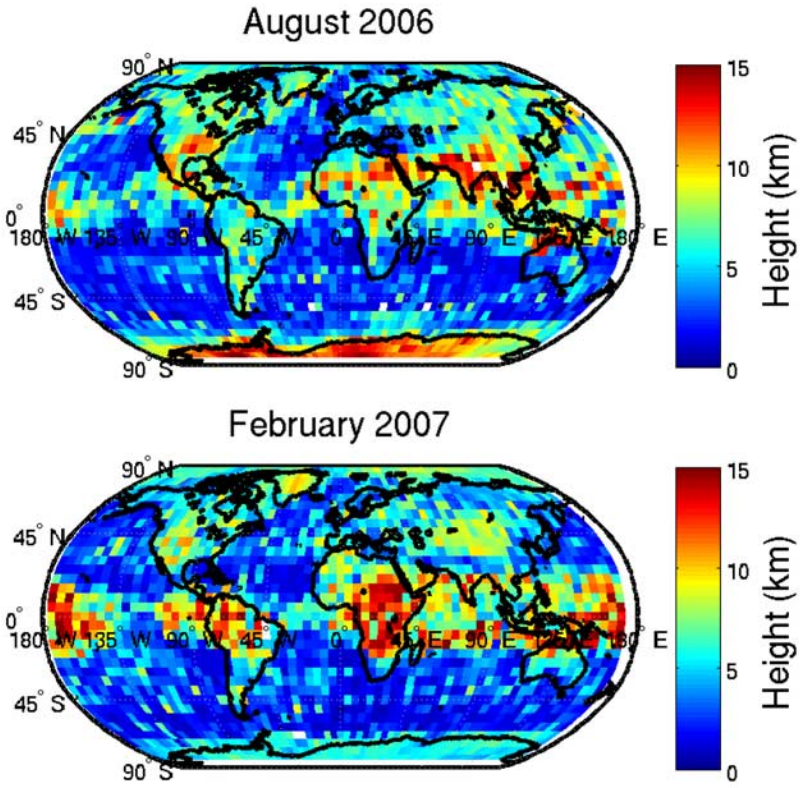

Figure 5. Average 5-km averaged CALIOP derived cloud height over a 5-degree region when the MODIS misses clouds detected by CALIOP.

tion in regions near the intertropical convergence zone (Figure 4) is likely due to optically thin cirrus that is undetected by MODIS (Figure 5). The disagreements in labeling a scene as cloudy also occur over the tropical deserts, caused by MODIS missing high thin cirrus and misclassification of aerosols as clouds by CALIOP. While the fraction of disagreement is large, the number of cases of cloudy scenes is generally small in comparison to other geographic regions. The next section further explores the differences the two approaches to cloud height.

3.2. Detecting High and Low Clouds

[33] Figure 5 shows the mean CTH, as determined by the CALIOP 5-km product, for cases when CALIOP detects a cloud and MODIS does not. This categorization reveals that differences in the tropical regions generally occur with high cloud. Disagreement in the summer monsoon region in August also is associated with high-level clouds, where the CALIOP has a greater sensitivity. The disagreement over the Siberian region in February occurs for clouds below 5 km. Also notice that during the Antarctic winter the mean cloud height of missed clouds is very high (15 km) and results from MODIS being insensitive to polar stratospheric clouds. A histogram of the CTH missed by MODIS is presented in Figure 6, with the results separated by the surface type. Over ocean the cloud mask primarily disagrees for low-level clouds while over land, the CTH distribution is more evenly distributed between high and low clouds. Over ocean, the disagreement between MODIS and CALIOP for low clouds occurs during both day and night, and can be attributed in part to spatial sampling differences for subpixel-scale cumulus. Investigation of individual granules supports this conclusion. An example subpixel-scale sampling differences is presented in Figure 1 with MODIS 1 km and CALIOP sampling overlaid over an observed 250 m MODIS reflectance image. Figure 6 reveals that for desert regions there are two modes in the missed CTH distribution; one peaks at 3 km and the other at 7 km. Investigation of

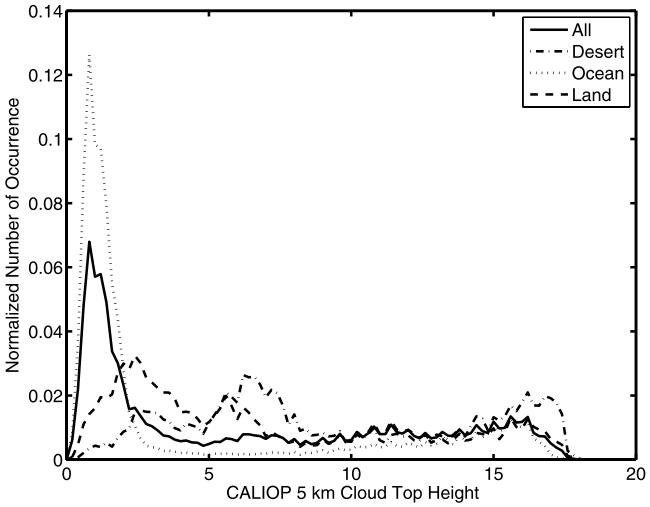

Figure 6. Normalized histogram of the CALIOP measured cloud top height for cases when the MODIS 1-km cloud mask misidentified the GIFOV as clear. The histograms are separated by the MODIS cloud mask land classification.

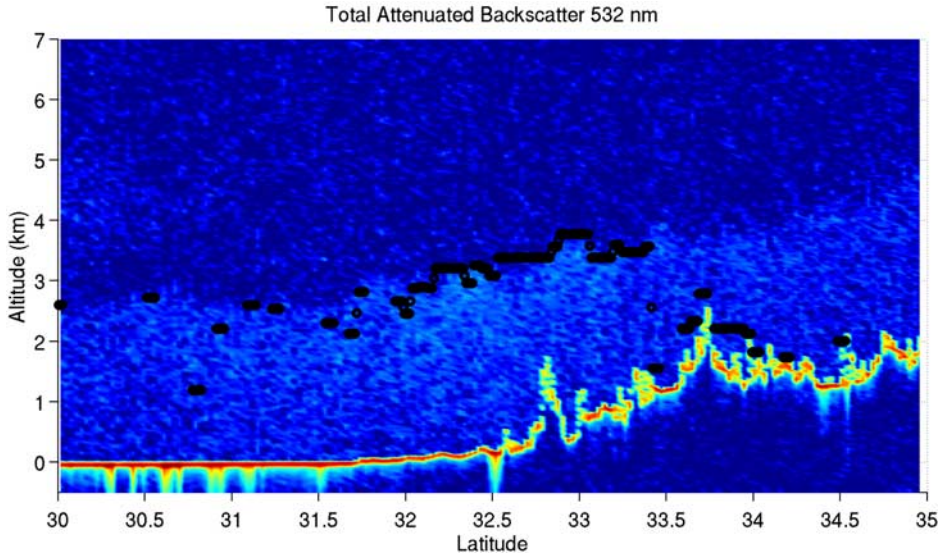

Figure 7. CALIOP attenuated backscatter profile with the CALIOP 5-km cloud top heights presented as black dots. Notice that CALIOP misidentifies the aerosol layer as cloud.

individual granules reveals that the higher mode in the desert distribution results from cases when the MODIS cloud mask misses thin cirrus. The lower mode at 3 km results from CALIOP incorrectly identifying thick aerosol layers as cloud with an example presented in Figure 7. This finding highlights the importance of considering the uncertainties in the evaluation measurements (CALIOP) when interpreting the comparison results.

3.3. Cloud Top Height

[34] Collocated 1-km and 5-km CALIOP CTH retrievals are compared with the MODIS 5-km cloud top pressure retrievals. Interpretation of the results is complex, with biases and uncertainties resulting from a combination of CALIOP and MODIS cloud sensitivity differences, systematic algorithm biases from MODIS and CALIOP, as well as uncertainties resulting from spatial sampling differences.

[35] As earlier discussed (section 2) either one or two CALIOP 5-km averaged CTH retrievals can fall within a single 5-km MODIS cloud top pressure retrieval. It is the averaged CALIOP CTH that is compared to the MODIS product. Even with an accurate collocation, CALIOP only samples a small fraction of the MODIS 5-km pixel array as shown in Figure 1a; introducing random uncertainty. To compare the MODIS CTP to the CALIOP cloud top height retrieval, the MODIS CTP is converted to CTH using a model profile. The difference between MODIS and CALIOP (MODIS - CALIOP) is calculated using the MODIS CTH and the mean of the collocated CALIOP CTH within the MODIS 5-km FOV.

[36] On the basis of this approach, CTH retrievals are collocated, and the CTH differences compared, for August 2006 and February 2007. The mean collocated CTH differences are presented in Table 4 with results separated by both CALIOP 1-km and 5-km layer averaging, high and low clouds, and global and nonpolar averages. For all nonpolar regions, the CTH differences are negative; suggesting that on average the CTH retrieved by MODIS is less than CALIOP. This negative difference is most pronounced for the CALIOP 5-km averaged cloud top heights which have the highest sensitivity to optically thin clouds. For high clouds (i.e., CTH > 5 km), the nonpolar mean CTH difference is −4.5 ± 4.6 km, a considerably larger absolute

Table 4. Cloud Top Height Global Statistics of the Mean Differences Between MODIS and CALIOP[a]

	August 2006 Mean ± STD (km)	February 2007 Mean ± STD (km)
Global 1 km (5 km)		
All clouds	−1.4 (−2.6) ± 2.9 (3.9)	−1.4(−2.6) ± 2.9(3.9)
High (>5 km)	−2.7 (−4.3) ± 2.9 (4.3)	−2.7 (−4.4) ± 3.5(4.4)
Low (<5 km)	−0.1 (−0.3) ± 1.3(1.3)	−0.3 (−0.4) ± 1.3(1.3)
Nonpolar (−60°–60° latitude)		
All Clouds	−1.5 (−2.8) ± 3.0(4.1)	−1.5(−2.8) ± 3.0(4.2)
High (>5 km)	−2.7 (−4.5) ± 3.7(4.6)	−2.7 (−4.5) ± 3.7(4.8)
Low (<5 km)	−0.3 (−0.4) ± 1.3(1.2)	−0.3 (−0.5) ± 1.3(1.3)
Arctic (>60° latitude)		
All Clouds	−0.7 (−1.7) ± 2.1(2.8)	−1.7 (−2.4) ± 2.7(3.0)
High (>4 km)	−1.5 (−2.8) ± 2.3(2.9)	−3.4 (−3.9) ± 2.4(2.6)
Low (<4 km)	0.3 (0.2) ± 1.2(1.2)	0.1(0.0) ± 1.7(1.7)
Northern midlatitude (25°–60° lat)		
All clouds	−1.3 (−2.4) ± 2.8(3.7)	−1.4 (−2.1) ± 2.4(2.8)
High (>5 km)	−2.2 (−3.7) ± 3.5 (4.1)	−2.3(−3.1) ± 2.7(3.1)
Low (<5 km)	−0.1 (−0.3) ± 1.4 (1.3)	−0.4(−0.6) ± 1.3(1.3)
Tropics (−25°–25° latitude)		
All clouds	−1.9 (−3.7) ± 3.6 (5.0)	−2.2(−4.1) ± 3.8(5.4)
High (>4 km)	−3.4 (−5.9) ± 4.4 (5.4)	−3.4(−6.2) ± 4.5(5.7)
Low (<5 km)	−0.4 (−0.6) ± 1.3(1.3)	−0.6(−0.8) ± 1.3(1.1)
Southern midlatitudes (−60°–−25° latitude)		
All clouds	−1.1 (−1.8) ± 2.2 (2.7)	−0.8(−1.6) ± 2.3(3.0)
High (>5 km)	−2.3 (−3.2) ± 2.6 (5.4)	−2.1(−3.3) ± 2.9(3.6)
Low (<5 km)	−0.3 (0.4) ± 1.1 (1.1)	0.0(−0.2) ± 1.3(1.2)
Antarctic < −60° latitude 1 km (5 km)		
All clouds	−1.9 (−3.2) ± 2.8(3.6)	−0.7 (−1.3) ± 1.7(2.2)
High (>4 km)	−3.1 (−4.4) ± 2.6(3.4)	−1.6 (−2.5) ± 1.9(2.3)
Low (<4 km)	0.5 (0.4) ± 1.4(1.4)	0.1 (0.0) ± 1.0(1.0)

[a]A mean less than zero occurs if the MODIS cloud top height is on average lower than CALIOP. The results are separated by month, global, and nonpolar with nonpolar including all regions except those above 60°N and below 60°S and polar regions. The results are also separated by 1-km and 5-km CALIOP cloud top heights with the 5-km differences within the parentheses.

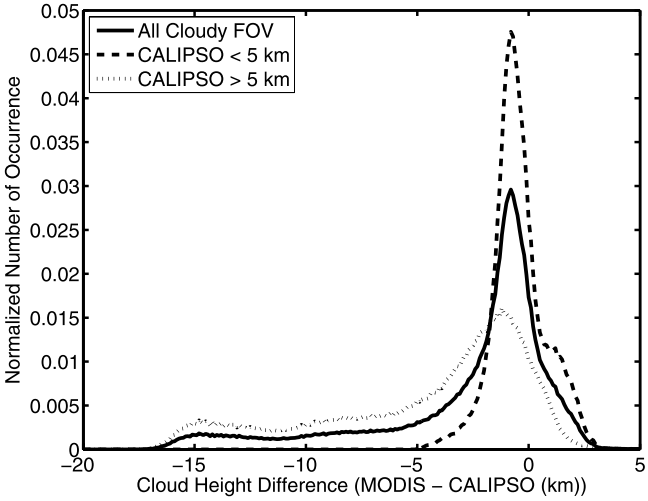

Figure 8. Normalized histogram of the global cloud height differences between MODIS and CALIOP for August 2006. The polar regions (60° latitude) have been excluded from the comparison. A negative difference occurs if the MODIS cloud top height is below CALIOP. The solid black distribution includes both high and low clouds. The red and blue distribution have been separated into high and low clouds, respectively. The distributions include over 2.4 million collocated comparisons.

difference than reported in previous aircraft studies [*Frey et al.*, 1999; *Holz et al.*, 2006]. The CTH difference changes significantly when comparing MODIS CTH to the 1-km averaged CALIOP CTH; a bias of −2.7 ± 3.7 km is found for August 2006, representing a change of more than 30%. For low clouds, (i.e., CTH < 5 km), the nonpolar mean global CTH differences are −0.4 ± 1.2 km, significantly smaller.

[37] To further investigate the global mean CTH differences, a histogram of the CTH differences is presented in Figure 8 between MODIS and the 5-km CALIOP products. The distribution encompassed by the solid black line includes all collocated nonpolar data where both CALIOP and MODIS retrieved a CTH. This distribution has a prominent peak just less than zero with a pronounced tail extending to beyond −15 km. There are a significant number of comparisons where MODIS retrieves a CTH higher than CALIOP in the distribution (a positive difference in the histogram).

[38] On the basis of the CALIOP CTH retrieval, the distribution was separated by low (<5 km) and high (>5 km) clouds as presented by the dashed distributions in Figure 8. The large negative differences are associated with high clouds. The pronounced positive "bump" at +1 km is associated with low-level clouds.

[39] Both the CALIOP and MODIS CTH retrievals are sensitive to the cloud optical properties and the local surface and atmospheric conditions. These characteristics have

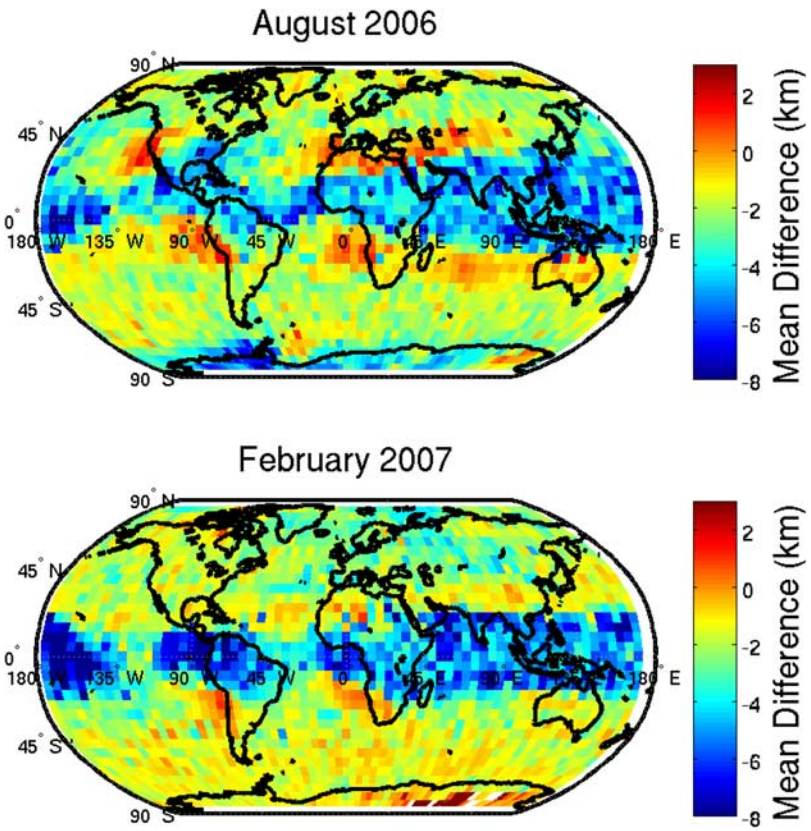

Figure 9. A 5-degree grid of the mean cloud top height differences are presented. For each 5-degree grid box the mean of all the collocated differences (MODIS – CALIOP) is calculated. A negative difference (blue) results when the mean MODIS cloud height is below the CALIOP, while the red values represent MODIS overestimating the cloud top height relative to CALIOP.

Table 5. Fractional Cloud Detection Agreement and Mean Cloud Top Height and Standard Deviation of the Differences Between MODIS and CALIOP for the Month of August 2006 for Clouds With Heights Greater than 5 km as Determined by CALIOP[a]

	All CALIOP Clouds CTH > 5 km X, Mean ± STD	CALIOP Attenuated CTH > 5 km X, Mean ± STD	CALIOP Not Attenuated CTH > 5km X, Mean ± STD
Nonpolar	0.90, −4.5 ± 4.7 km	1.00, −1.0 ± 1.6 km	0.88, −5.2 ± 4.7 km
Arctic	0.92, −2.8 ± 2.9 km	0.99, −0.3 ± 1.5 km	0.91, −3.4 ± 2.8 km
North midlatitudes	0.85, −3.7 ± 4.1 km	0.99, −0.7 ± 1.6.km	0.84, −4.3 ± 4.2 km
Tropics	0.88, −5.9 ± 5.4 km	1.00, −1.1 ± 1.8 km	0.87, −6.6 ± 5.4 km
South midlatitudes	0.97, −3.2 ± 3.1 km	1.00, −1.1 ± 1.5 km	0.96, −3.9 ± 3.2 km
Antarctica	0.72, −4.4 ± 3.4 km	0.95, −2.3 ± 2.5 km	0.70, −4.7 ± 3.4 km

[a]X denotes fractional cloud detection agreement. Results are separated by cases when CALIOP was and was not attenuated by the first cloud layer.

strong regional dependencies that are evident in our analysis of the monthly global data. Figure 9 presents the collocated mean CTH differences separated into 5° grid boxes for August 2006 and February 2007. Each grid cell presents the mean CTH differences for all the collocated MODIS/CALIOP data within the cell.

[40] Figure 9 reveals a significant geographical dependence in the CTH differences found in Figure 8. The large underestimation of the MODIS CTH for high clouds is strongly correlated with latitude, with mean CTH differences greater than 6 km near the Intertropical Convergence Zone (ITCZ) for August 2006. This region has a considerable amount of optically thin cirrus during the northern hemisphere summer. The region of negative CTH differences migrates slightly south during February 2007 with a more pronounced region of large negative differences found over northern South America and the Western Pacific. The mean cloud height differences for high tropical clouds is found to be −5.9 ± 5.4 km with the largest differences for nonopaque clouds with mean differences of −6.6 ± 5.4 km as presented in Table 5. The CTH agreement improves near Florida and the Caribbean in February, likely resulting from the decrease in convection during the winter months. Significant CTH differences are found in the polar regions, with MODIS significantly underestimating the CTH relative to CALIOP over much of the Antarctic during winter (August 2006). The magnitude of the polar disagreement lessens considerably in February due largely to a substantial increase in the MODIS overestimation of the CTH (Antarctic summer).

3.4. Comparison for Marine Low-Level Clouds

[41] The systematic MODIS CTH overestimation in Figure 9 is most pronounced off the North American Pacific coast, the west coast of South America and off the Eastern coast of Southern Africa. These three regions have a frequent occurrence of marine stratus and stratocumulus clouds. To investigate this bias, the MODIS CTH is compared to the CALIOP attenuated backscatter profiles with an example presented in Figure 10. For the regions with a high bias (>1 km), the mean MODIS CTH retrievals are approximately 1.5 km above the CALIOP-based CTH. The possible presence of thin cirrus above the lower water cloud layer could explain the MODIS overestimation; however, cirrus is notably absent in the CALIOP attenuated backscatter data. Further investigation of the MODIS CTP retrieval algorithm revealed that overestimation occurs in regions with low-level temperature inversions. In the Collection-5 operational retrieval approach, the 11-μm window Brightness Temperature (BT) is matched to that calculated using the GDAS temperature and water vapor profile. The algorithm searches the model profile from the troposphere to the surface (i.e., a top-down approach). The first match in brightness temperature provides the CTP. In the presence of a temperature inversion, there may be multiple solutions for the CTP. Marine stratus frequently occurs near the bottom of a

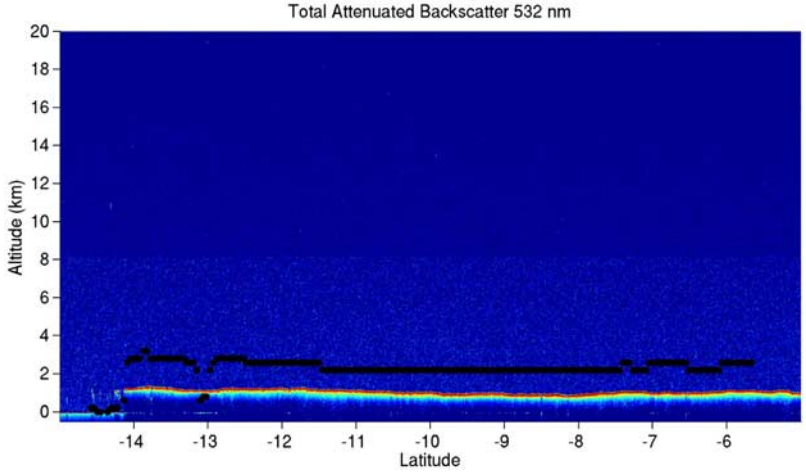

Figure 10. CALIOP attenuated backscatter profile of Marine stratus from 24 August 2006 off the coast of South America. The black dots are the collocated MODIS cloud height retrieval.

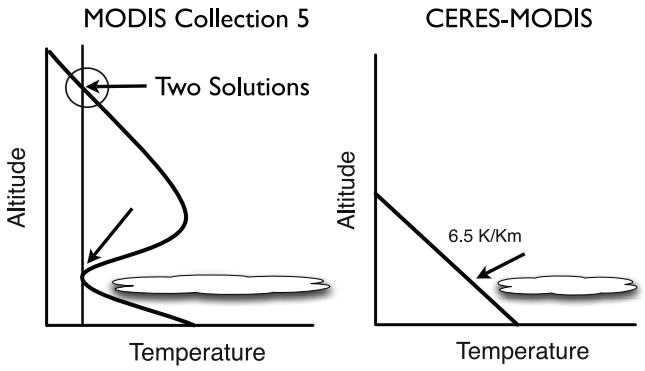

Figure 11. A graphical representation of the MODIS Collection-5 window BT retrieval over (left) marine stratus and (right) the CERES methodology. The Collection-5 retrieval typically selects the window BT intersection circled in the left panel.

temperature inversion as depicted in Figure 11. Because the current MODIS algorithm selects the temperature intersection at the top of the inversion, the CTP is underestimated.

[42] As part of the University of Wisconsin Product Evaluation and Test Element (PEATE), the MODIS Collection-5 cloud top height retrieval was modified to use the marine stratus retrieval algorithm given by [*Minnis et al.*, 1992], which assumes a constant lapse rate normalized to the GDAS ocean surface temperature. The MODIS Collection-5 algorithm was reprocessed with the modified retrieval and then reevaluated using CALIOP for August 2006 with the results presented in Figure 12. The revised MODIS CTH assignment for low clouds yields significantly improved comparisons with CALIOP with a mean difference of −0.2 km.

3.5. Comparisons for MODIS High-Level Clouds (CTH > 5 km)

[43] A surprisingly large negative bias was found in Figure 8 for high clouds (CTH > 5 km). A negative bias can be expected for optically thin but geometrically thick cirrus, because the CO_2 slicing retrieval is sensitive to the cloud radiative mean pressure. For the case of an optically thin but geometrically thick cloud, the inferred CTH is expected to fall below the lidar-retrieved CTH [*Holz et al.*, 2006; *Naud et al.*, 2005]. For single-layered ice clouds, the expected CTH differences can be as large 5 km. However, these CTH differences are still considerably smaller than the differences found for the global distribution in Figure 8.

[44] Globally, the largest differences occur immediately north and south of the equator as shown in Figure 9. This region has frequent high thin cirrus, often with complex multilayered cloud formations. Table 5 presents the August 2006 mean cloud height differences for high clouds greater than 5 km, separated by latitude region and attenuating and nonattenuating clouds as determined by the CALIOP opacity flag. For attenuating tropical high clouds, the mean cloud height difference between CALIOP and

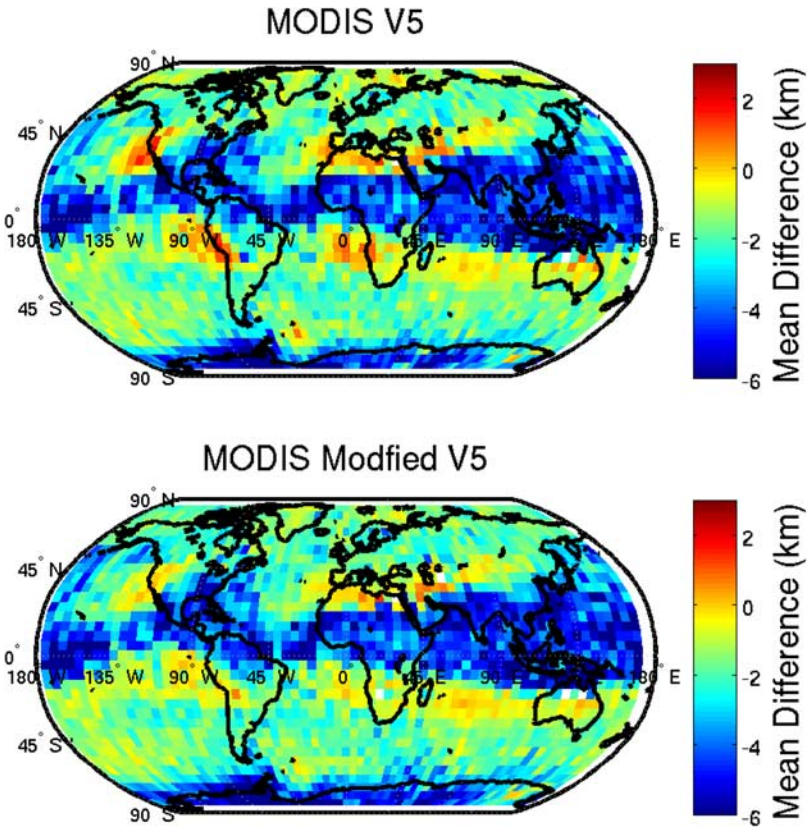

Figure 12. (top) The 5-degree grid of the mean differences between CALIOP and MODIS (MODIS – CALIOP) for the Collection-5 MODIS retrieval compared with (bottom) the modified marine stratus retrieval.

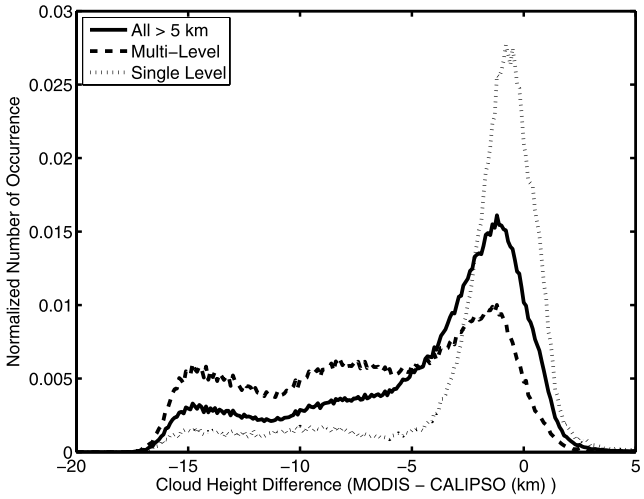

Figure 13. Histogram of global cloud height differences for August 2006 are presented filtered by single and multilayer clouds using CALIOP. A multilayer cloud is defined using CALIOP and requires that maximum cloud top height be greater than 5 km and the separation between the top cloud layer base and cloud top height of the bottom layer be greater than 4 km.

MODIS is approximately -1.1 ± 1.8 km in contrast to the nonattenuated cases with mean differences greater than -6.6 ± 5.4 km. Multilayered clouds can result in large cloud height underestimation when applying CO_2 slicing [*Baum and Wielicki*, 1994], providing possibly one explanation for the large negative bias for nonattenuating clouds. The impact of multilayered clouds on MODIS is investigated using the collocated CALIOP CTH retrievals. When the column optical thicknesses are less than approximately 3, CALIOP can accurately detect both base heights and top heights within multilayered cloud scenes. On the basis of the CALIOP 5-km layer product, the global data set was separated into both single-layered high clouds (CTH > 5 km) and multilayered clouds, with multilayered clouds being defined as having more than one cloud layer in a vertical column with at least one layer separated from another by more than 4 km from the nearest neighbor. Figure 13 presents the histogram for August 2006 for cloud height differences separated by single and multilevel clouds. When interpreting the results, it is important to consider CALIOP's sensitivity to multilayered clouds and the optical thickness limit. CALIOP is sensitive to a lower layer only if the signal is not totally attenuated by the upper layer(s). Because the MODIS sensitivity to multilayered clouds is also reduced as the optical thickness of the uppermost cloud layer increases, it is expected that the CALIOP multilayered cloud filter should be representative of the MODIS sensitivity. In Figure 13 the multilayered cloud histogram displays a significantly larger CTH bias then the single layer histogram indicating that multilayered clouds have a considerable impact on the MODIS CTH biases. However, even with the multilayered cases removed, the single-layered cloud histogram still has a considerable number of cases that show a large negative bias.

[45] Multilayered clouds do not fully explain the negative CTH biases found in Figure 8. The MODIS algorithm retrieval estimates the CTP/CTH using one of two methods. If the CO_2 slicing algorithm does not converge to an acceptable solution, the retrieval reverts to a water vapor corrected 11-μm window BT retrieval. If MODIS reverts to the window BT retrieval for cases with optically thin cirrus, a significant cloud top height underestimation can be expected [*Baum et al.*, 2003]. A limited comparison with ground-based measurements found that MODIS often reverts to an 11-um window retrieval for very thin cirrus resulting in significant biases [*Naud et al.*, 2004]. To investigate this impact, the collocated data set was separated on the basis of the MODIS retrieval method with results presented in Figure 14. For scenes when MODIS successfully applies CO_2 slicing, the distribution becomes considerably narrower, almost eliminating the very large negative CTH biases found in the distribution containing all MODIS CTH retrievals (window BT and CO_2 slicing). The mean bias compared to the CALIOP 5 km layer products for CO_2 slicing during August 2006 was -2.4 ± 2.8 km. For scenes determined by CALIOP to include single-layer clouds, the MODIS CO_2 slicing histogram is narrower than both the combined and CO_2-slicing-only results with a mean bias of -1.0 ± 1.8 and agrees with the expected biases resulting from the physical sensitivity differences between a passive IR-based and active sensor CTH retrieval [*Holz et al.*, 2006]. The accuracy of the MODIS CO_2 slicing retrieval can be perturbed by several external factors, including instrument noise, radiometric biases, and uncertainties in the calculated clear sky radiances. The ability of MODIS to retrieve an accurate cloud top height using CO_2 slicing thus depends on a combination of the uncertainties inherent in the retrieval process and the magnitude of the cloud signal present in the measured radiances. The cloud signal magnitude in turn depends primarily on the cloud top height and the cloud optical thickness. However, because estimates of cloud optical thickness are not presently available in the

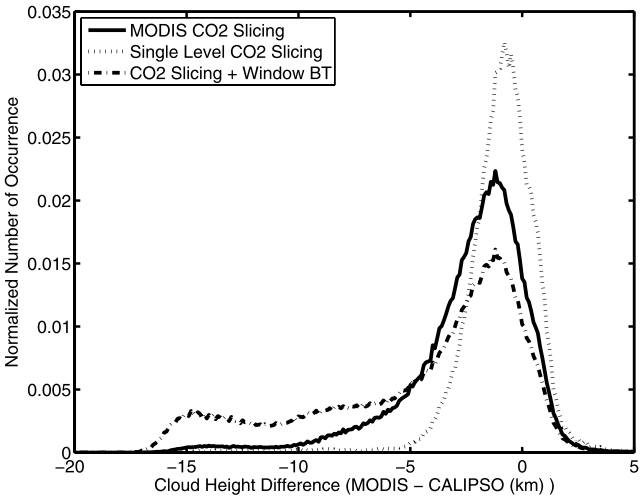

Figure 14. Histogram of the global cloud height differences during August 2006 for CALIOP determined high clouds (>5 km) filtered for cases where the MODIS retrieval applied CO_2 slicing (solid line) and CALIOP determined single level clouds (dotted line). The distribution for all high clouds (combined CO_2 slicing + window BT retrieval) is also presented.

CALIOP data stream, it is not possible to quantify the optical thickness limitations in the MODIS retrievals that contribute to the large negative biases. However, the results suggest that the MODIS CTH retrieval could be improved by applying CO_2 more often instead of the window BT retrieval for the thin cirrus. This remains an active area of investigation.

4. Conclusions

[46] This paper compares CALIOP and MODIS Collection 5 cloud detection and cloud top height (CTH) assignments. To facilitate the comparison an accurate collocation algorithm was developed. The comparison is conducted globally for the months of August 2006 and February 2007.

[47] For cloud detection, the two approaches (CALIOP and MODIS) agree on a scene being clear or cloudy over 75% of the time excluding the polar regions. However, the agreement is dependent on the methodology used in the comparison, including the collocation process and the CALIOP averaging approach. The agreement is generally better for cloudy scenes than clear. At regional scales, cloud detection differences can be significant, with the largest disagreements found in the polar and desert regions. Over deserts the disagreement results from MODIS missing high thin cirrus but also CALIOP incorrectly identifying thick aerosol layers as cloud. A small diurnal detection dependence is found, with, on average, 2–3% better agreement occurring for daytime measurements. Significant disagreement found in the Arctic and Antarctic regions, including the southern ocean near the sea ice boundary that is attributed to the highly variable surface emissivity of broken ice and the lack of contrast between the surface and clouds. Disagreement during the Antarctic winter can be partially attributed to polar stratospheric clouds that are detected by CALIOP but not MODIS.

[48] For CTH retrievals, the comparison reveals disagreements with a strong regional and cloud type dependence. A systematic high CTH bias of 1–2 km is found in the MODIS results for both August 2006 and February 2007 in oceanic regions with high frequencies of occurrence of stratocumulus. The cause of the bias is traced to the window BT cloud height retrieval in the MODIS Collection 5 algorithm, and is attributed to the approach used to infer CTH when low-level temperature inversions exist. The temperature profile near the surface was modified to a constant lapse rate, the MODIS data subsequently reprocessed, with results again compared to CALIOP for August 2006. The CTH bias was mitigated using the modified cloud retrieval approach. This correction will be implemented into the next version of the MODIS cloud software.

[49] For optically thin, but geometrically thick high clouds (CTH > 5 km), MODIS underestimates the CTH relative to CALIOP. When compared to the CALIOP 1-km averaged products, the nonpolar mean CTH difference between CALIOP and MODIS was found to be approximately 3 km for both August 2006 and February 2007. The 5-km CALIOP CTH products have mean differences with MODIS that are greater than 4 km. The larger bias for the CALIOP 5-km averages results from the sensor's increased sensitivity to optically thin cirrus. For cases when the first cloud layer did not attenuate CALIOP, the mean difference for high clouds for August 2006 was −6.6 km. The large CTH differences were investigated, with the largest differences found for high thin cirrus in the equatorial region with differences greater than 15 km. For these cases it was found that the MODIS reverted to a water vapor corrected window brightness temperature retrieval instead of using CO_2 slicing. When the differences were filtered to only include CO_2 slicing retrievals, the agreement improved significantly, with the best agreement when CO_2 slicing was applied to single layered clouds with a mean difference of -1.0 ± 1.9 km.

Appendix A

[50] A detailed description of the method developed to collocate MODIS with CALIOP is presented. The algorithm is designed to be computationally efficient and accurate allowing for rapid identification of the coincident CALIOP and MODIS observations. Before proceeding to describe the details of the collocation algorithm we need to first define the coordinate systems in use. No explanation needs to be given of latitude and longitude, except to point out that latitudes must be distinguished as either geodetic or geocentric, and that failure to do so leads to errors that vitiate any results. Neglecting this distinction can lead to a maximum error of about 21 km. The celestial coordinate system, which some may refer to as inertial, has its origin at the center of the Earth, its x axis in the equatorial plane directed toward the Vernal Equinox, its y axis 90 degrees to the east of the Vernal Equinox, and the z axis through the North Pole. This basis is fixed to the heavens, and points of the Earth change their celestial coordinates continually as the Earth rotates. The terrestrial coordinate system is fixed to the rotating Earth, with the x axis in the plane of the equator directed toward the Greenwich meridian, and y axis 90 degrees to the east, and the z axis again through the North Pole. Knowledge of the longitude of the Vernal Equinox as a function of time allows easy conversion between celestial and terrestrial frames. Simple trigonometry allows conversion between geocentric latitude/longitude and the terrestrial frame. Conversions between geodetic and geocentric latitude can use the relation

$$b^2 \tan D = \tan C,$$

where $b^2 = 0.99327730$, and where D and C are geodetic and geocentric latitude, respectively.

[51] Suppose that we are given a single MODIS scan line containing 1354 points, the Earth locations of which are provided. We seek to know which of a large number of CALIOP GIFOV intersect this MODIS scan line. We suppose further that these MODIS locations are in the form of geodetic latitude, longitude, and a corresponding time. Our task is to determine which of the 1354 FOVs on this scan line coincide with which of the roughly 65000 FOVs in the CALIOP data set, a total of about 9×107 possible overlaps to be checked. A tedious computer search to ascertain these overlaps is undesirable, whereas the collocation algorithm allows us to restrict the point-by-point search to a mere handful of MODIS and CALIOP observations. At a bare minimum, before undertaking any search, one would at least wish to ascertain that the MODIS scan

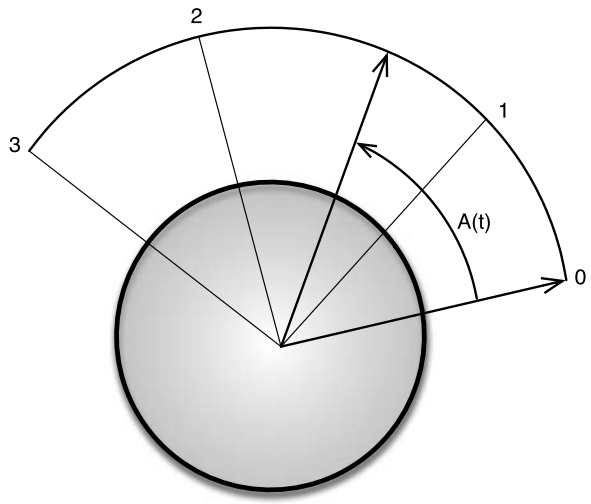

Figure A1. Knowledge of a satellite's angular displacement at four points along an orbital segment allows us to express its instantaneous displacement as a cubic polynomial. Being differentiable, the polynomial can be numerically inverted to find the time of a given displacement.

line and the CALIOP traces even intersect. In the following, we shall disregard terrain elevation, with the understanding that its consideration is not a major complication.

[52] The given MODIS scan line does not describe a great circle across the face of the Earth. The satellite moves and the Earth rotates during the time required to make the scan (less than 0.5 s). Moreover, the satellite when looking at nadir may not be looking directly toward the center of the Earth, but rather looking normal to the Earth's underlying surface. But because the satellite's motion during the scan is on the order of 3 kilometers, and the movement of a point of the Earth is at most 0.231 km during the scan, we make the slightly inaccurate assumption that the MODIS scan across the Earth is a great circle in the terrestrial system described by the vector cross product

$$\mathbf{M} = \mathbf{A} \times \mathbf{B},$$

where **A** and **B** are the initial and final MODIS scan position vectors, with the center of the Earth as origin, and **M** is the vector quasi-plane of the scan. Since MODIS scans from right to left, the vector **M** is oriented backward along the MODIS subsatellite track.

[53] Consider next the trace of the CALIOP nadir-viewing instrument across the Earth. Both CALIPSO and AQUA are sun-synchronous satellites. The right ascension of there ascending nodes precess about 360 degrees in 365 days, or about 0.07 degrees per orbit. Hence over a fraction of an orbit, we can consider the satellite's motion to lie in a quasi-plane in the celestial coordinate system, which simplifies the task of estimating its motion in the absence of its orbital parameters. The Earth-located points which lie along the CALIOP path have a time associated with each, and can hence be converted to celestial coordinates. Two cubic polynomials with time as the independent variable, computed from four points chosen at roughly equal intervals along the CALIOP path, enable us to estimate both the angular displacement of the CALIOP satellite from the first CALIOP point, and the satellite's radius vector from the center of the Earth, in the celestial frame. For instance, we can compute the coefficients of a cubic polynomial which expresses the satellite's arc distance A from some initial position vector (e.g., the first CALIOP position) within the quasi-plane of the satellite's orbit, and within a limited time span (e.g., 25 min), as a function of time

$$A(t) = C_0 + C_1 t + C_2 t^2 + C_3 t^4,$$

where A(t) is the angular displacement from an initial time.

[54] *Froberg* [1965] has suggested a simple means of computing such polynomials. The four times needed to compute these coefficients are normally provided with the MODIS and CALIOP data sets, and the four needed values of arc distance are likewise inferred from the Earth-located CALIOP data (see Figure A1). A polynomial is differentiable and therefore the above can be inverted to obtain t, given arc length, by a Newton-Raphson successive approximation

$$t_1 = t_0 - A(t)/A'(t),$$

where the iteration continues until some threshold is reached. (A Newton-Raphson technique is valid for finding real roots of a polynomial A(t) provided the polynomial does not have a repeated root within the region of interest which would cause its derivative $A'(t)$ to vanish at that root.) We now have a scheme for inverse navigation; that is, the ability to compute the time when a satellite (e.g., CALIOP) will be over or abeam of a given point (e.g., a MODIS FOV) on the Earth, and hence we know approximately the CALIOP observation closest to the given MODIS FOV. Somewhat less importantly, a similar polynomial can be used to express the scalar radius vector of a satellite within the same time interval.

[55] These two polynomials can serve for inverse navigation, allowing us to estimate the time when CALIOP is over a given point on the Earth surface. Finally, these polynomials can be differentiated to obtain satellite velocity. We might add that it is by no means necessary to use polynomials as a simple navigation model. One could, for instance, create a table of satellite positions directly from the data files, separated by small time intervals, and interpolate directly into these tables. Polynomials, however, by being easily differentiable, provide a simple means of both forward and inverse navigation, and for estimating velocity.

[56] The subsatellite track created by CALIOP points is certainly not a great circle when plotted on the Earth, but this path is nearly a great circle in celestial space. The path of the satellite over the ground is the projection of its path through space, adjusted to correct for the satellite's apparent westward movement by virtue of the Earth's eastward rotation. If we choose an arbitrary CALIOP FOV from the given CALIOP set as a first guess for the one overlapping the given MODIS scan, then the satellite's apparent velocity with respect to the Earth at that FOV is its velocity through space, obtained by differentiating our polynomials for satellite position, adjusted by the eastward movement of the underlying Earth, i.e.,

$$\mathbf{V}_t = \mathbf{V}_s - E\cos(L)\mathbf{U}_e,$$

where the vector $\mathbf{V_t}$ is terrestrial satellite velocity, $\mathbf{V_s}$ is the velocity through space diminished by the ratio of Earth radius to satellite radius vector, and $\mathbf{U_e}$ is a unit vector pointing toward local east at the given FOV. The scalar E is the eastward speed of the Earth's rotation at the equator. The vector osculating plane of the satellite's movement in terrestrial space is given by

$$\mathbf{P} = \mathbf{R} \times \mathbf{V}_t,$$

where $\mathbf{R}$ is the terrestrial position vector of the chosen FOV. This osculating plane contains the CALIOP's instantaneous velocity vector in the terrestrial frame at the chosen FOV with respect to the underlying Earth. The cross product of the two terrestrial vectors $\mathbf{P}$ and $\mathbf{M}$ points approximately to the intersection on the Earth's surface of these two planes, which is roughly the point at which the CALIOP trace intersects the given MODIS scan line. The initially chosen CALIOP FOV may be far removed from this intersection, and hence the CALIOP/MODIS intersection may be erroneous. However, we can inverse-navigate the CALIPSO satellite to find the time when it is over this conjectural intersection, and we now have a more accurate estimate of the CALIOP FOV closest to the MODIS scan. We can hence iterate the procedure, thus obtaining a more accurate fix on the MODIS/CALIPSO intersection, etc., until some criterion is satisfied. At length we need only search for a few MODIS and a few CALIOP FOVs to find the ones that precisely overlap.

[57] Further iterations of this scheme for subsequent MODIS scan lines are more rapid since we already have an excellent first guess for the CALIOP point which overlies the next MODIS scan line.

[58] The question of ascertaining whether a CALIOP FOV actually overlies a given MODIS FOV may be viewed as follows: The CALIOP is a nadir-viewing instrument, but the MODIS scanner may view a particular MODIS FOV at an angle which departs significantly from nadir. In such a case the MODIS FOV, projected onto the ground, is quasi-elliptical rather than circular. Let us deal first with this case.

[59] If r is the nominal radius of the MODIS FOV at nadir, then the semiminor axis of an elliptical FOV is

$$m = rs/h,$$

where s is the slant range from satellite to the FOV, and h is the altitude of the MODIS-carrying spacecraft. We define the unit vector $\mathbf{j}$ as the cross product

$$\mathbf{j} = U(\mathbf{R} \times \mathbf{S}),$$

where $\mathbf{R}$ is the position vector of the MODIS FOV, and $\mathbf{S}$ is the slant range vector from the MODIS FOV to the AQUA satellite. The operator U is a normalizing operator that reduces its vector argument to unit length. The vector semiminor axis is thus m$\mathbf{j}$. The semimajor axis of the FOV lies along the unit vector $\mathbf{i}$ and is given by

$$\mathbf{i} = U(\mathbf{j} \times \mathbf{S}),$$

and the vector semimajor axis is $\mathbf{M}$ = m sec(A)$\mathbf{i}$; that is, it has the length of the semiminor axis elongated by the secant of the azimuth angle A. If $\mathbf{C}$ is the vector position of a CALIOP observation, then the x and y coordinates of a CALIOP point relative to the center of the elliptical MODIS FOV are the dot products

$$x = (\mathbf{C} - \mathbf{R})^* \mathbf{i}$$

$$y = (\mathbf{C} - \mathbf{R})^* \mathbf{j}.$$

The radial distance r^2 is given by the Pythagorean theorem $r^2 = x^2 + y^2$. If r^2 is less than m^2, the semiminor axis, then the CALIOP observation lies within the MODIS oval. If it is greater than M^2, the semimajor axis, it lies outside. In the intermediate case, if

$$y^2 < m^2\left(1 - x^2/M^2\right),$$

it lies inside, and in this event we assign to the CALIOP observation a weight

$$w = 1 - \left(x^2 + y^2\right)/\left(x^2 + m^2\left(1 - x^2/M^2\right)\right).$$

This weight is one if x, y = 0, i.e., the CALIOP point lies at the dead center of the MODIS FOV, and the weight is zero if it lies at the periphery of the MODIS FOV.

[60] It may happen that the MODIS FOV lies at or near the nadir of the AQUA, in which case we simply treat the MODIS FOV as if it were a circle with nominal nadir radius.

[61] **Acknowledgments.** We would like to acknowledge the NASA atmospheric Product Evaluation and Test Element for supporting this research. We would like to thank Liam Gumley, Scott Mindock, and Paul Menzel for their support. This research was funded under NASA grants NNG04HZ38C, NAS1–99106, and NNX07AR95G; NNG05GN47A also contributed to this study. We would also like to thank the MODIS and CALIPSO teams for supplying the data used in for this research.

References

Abshire, J., X. Sun, H. Riris, J. M. Sirota, J. F. McGarry, S. Palm, D. Yi, and P. Liiva (2005), Geoscience Laser Altimeter System (GLAS) on the ICESat mission: On-orbit measurement performance, *Geophys. Res. Lett.*, *32*, L21S02, doi:10.1029/2005GL024028.

Ackerman, S. A., K. I. Stabala, W. P. Menzel, R. A. Frey, C. Moeller, and L. E. Gumley (1998), Discriminating clear sky from clouds with MODIS, *J. Geophys. Res.*, *103*, 32,141–32,157, doi:10.1029/1998JD200032.

Ackerman, S. A., R. E. Holz, R. Frey, E. W. Eloranta, B. Maddux, and M. J. McGill (2008), Cloud detection with MODIS: Part II. Validation, *J. Atmos. Oceanic Technol.*, *25*, 1073–1086.

Baum, B. A., and B. Wielicki (1994), Cirrus cloud retrieval using infrared sounding data: Multilevel cloud errors, *J. Appl. Meteorol.*, *33*, 107–117, doi:10.1175/1520-0450(1994)033<0107:CCRUIS>2.0.CO;2.

Baum, B. A., R. A. Frey, G. G. Mace, M. K. Harkey, and P. Yang (2003), Nighttime multilayered cloud detection using MODIS and ARM data, *J. Appl. Meteorol.*, *42*, 905–919, doi:10.1175/1520-0450(2003)042<0905:NMCDUM>2.0.CO;2.

Frey, R. A., B. A. Baum, W. P. Menzel, S. A. Ackerman, C. C. Moeller, and J. D. Spinhirne (1999), A comparison of cloud top heights computed from airborne lidar and MAS radiance data using CO_2 slicing, *J. Geophys. Res.*, *104*, 24,547–24,555, doi:10.1029/1999JD900796.

Frey, R., S. A. Ackerman, Y. Liu, K. I. Strabala, H. Zhang, J. Key, and X. Wang (2008), Cloud detection with MODIS: Part I. Improvements in the MODIS Cloud Mask for Collection 5, *J. Atmos. Oceanic Technol.*, *25*, 1057–1072.

Froberg, C. E. (1965), *Introduction to Numerical Analysis*, Addison-Wesley, New York.

Hawkinson, J. A., W. Feltz, and S. A. Ackerman (2005), A comparison of GOES sounder- and cloud lidar- and radar-retrieved cloud-top heights, *J. Appl. Meteorol.*, *44*, 1234–1242, doi:10.1175/JAM2269.1.

Heidinger, A. K. (2003), Rapid day-time estimation of cloud properties over a large area from radiance distributions, *J. Atmos. Oceanic Technol.*, *20*, 1237–1250, doi:10.1175/1520-0426(2003)020<1237:RDEOCP>2.0.CO;2.

Holz, R. E., S. Ackerman, P. Antonelli, F. Nagle, R. O. Knuteson, M. McGill, D. L. Hlavka, and W. D. Hart (2006), An improvement to the high-spectral-resolution CO_2-slicing cloud-top altitude retrieval, *J. Atmos. Oceanic Technol.*, *23*, 653–670, doi:10.1175/JTECH1877.1.

Kahn, B. H., A. Eldering, A. J. Braverman, E. J. Fetzer, J. H. Jiang, E. Fishbein, and D. L. Wu (2007a), Towards the characterization of upper tropospheric clouds using Atmospheric Infrared Sounder and Microwave Limb Sounder observations, *J. Geophys. Res.*, *112*, D05202, doi:10.1029/2006JD007336.

Kahn, B. H., et al. (2007b), Cloud-type comparison of AIRS, CloudSat, and CALIPSO cloud height and amount, *Atmos. Chem. Phys. Discuss.*, *7*, 13,915–13,958.

King, M. D., W. P. Menzel, Y. J. Kaufman, D. Tanre, B. C. Gao, S. Platnick, S. A. Ackerman, L. A. Remer, R. Pincus, and P. A. Hubanks (2003), Cloud and aerosol properties, precipitable water, and profiles of temperature and humidity from MODIS, *IEEE Trans. Geosci. Remote Sens.*, *41*, 442–458, doi:10.1109/TGRS.2002.808226.

Liu, Z., M. A. Vaughan, D. M. Winker, C. A. Hostetler, L. R. Poole, D. L. Hlavka, W. Hart, and M. McGill (2004), Use of probability distribution functions for discriminating between cloud and aerosol in lidar backscatter data, *J. Geophys. Res.*, *109*, D15202, doi:10.1029/2004JD004732.

Mahesh, A., M. A. Gray, S. Palm, W. Hart, and J. D. Spinehirne (2004), Passive and active detection of clouds: Comparisons between MODIS and GLAS observations, *Geophys. Res. Lett.*, *31*, L04108, doi:10.1029/2003GL018859.

Menzel, W. P., F. Richard, H. Zhang, D. P. Wylie, C. Moeller, R. E. Holz, B. Maddux, K. I. Strabala, and L. E. Gumley (2008), MODIS global cloud-top pressure and amount estimation: Algorithm description and results, *J. Appl. Meteorol. Climatol.*, *47*, 1175–1198, doi:10.1175/2007JAMC1705.1.

Min, Q., P. J. Minnett, and M. M. Khaiyer (2004), Comparison of cirrus optical depths derived from GOES 8 and surface measurements, *J. Geophys. Res.*, *109*, D15207, doi:10.1029/2003JD004390.

Minnis, P., P. W. Heck, D. F. Young, C. W. Fairall, and J. Snider (1992), Simultaneous satellite and island-based instrumentation during FIRE, *J. Appl. Meteorol.*, *31*, 317–339, doi:10.1175/1520-0450(1992)031<0317:SCPDFS>2.0.CO;2.

Naud, C., J. Muller, M. Haeffelin, Y. Morille, and A. Delaval (2004), Assessment of MISR and MODIS cloud top heights through inter-comparison with a back-scattering lidar at SIRTA, *Geophys. Res. Lett.*, *31*, L04114, doi:10.1029/2003GL018976.

Naud, C., J. Muller, and P. de Valk (2005), On the use of ICESAT-GLAS measurements for MODIS and SEVIRI cloud-top height accuracy assessment, *Geophys. Res. Lett.*, *32*, L19815, doi:10.1029/2005GL023275.

Platnick, S., M. D. King, S. A. Ackerman, W. P. Menzel, B. A. Baum, J. C. Riedi, and R. A. Frey (2003), The MODIS cloud products: Algorithms and examples from Terra, *IEEE Trans. Geosci. Remote Sens.*, *41*, 459–473.

Reagan, J. A., X. Wang, and M. T. Osborne (2002), Spaceborne lidar calibration from cirrus and molecular backscatter returns, *IEEE Trans. Geosci. Remote Sens.*, *40*, 2285–2290, doi:10.1109/TGRS.2002.802464.

Rossow, W. B., and R. A. Schiffer (1999), Advances in understanding clouds from ISCCP, *Bull. Am. Meteorol. Soc.*, *80*, 2261–2287, doi:10.1175/1520-0477(1999)080<2261:AIUCFI>2.0.CO;2.

Smith, W. L., and C. M. R. Platt (1978), Comparison of satellite-deduced cloud heights with indications from radiosonde and ground-based laser measurements, *J. Appl. Meteorol.*, *17*, 1796–1802, doi:10.1175/1520-0450(1978)017<1796:COSDCH>2.0.CO;2.

Stephens, G. L., et al. (2002), The CloudSat mission and the A-Train: A new dimension of space-based observations of clouds and precipitation, *Bull. Am. Meteorol. Soc.*, *83*, 1771–1790, doi:10.1175/BAMS-83-12-1771.

Thomas, A., et al. (2002), In situ measurements of background aerosol and subvisible cirrus in the tropical tropopause region, *J. Geophys. Res.*, *107*(D24), 4763, doi:10.1029/2001JD001385.

Vaughan, M. A., S. A. Young, D. M. Winker, K. Powell, A. Omar, Z. Liu, Y. X. Hu, and C. Hostetler (2004), Fully automated analysis of space-based lidar data: An overview of the CALIPSO retrieval algorithms and data products, *Proc. SPIE Int. Soc. Opt. Eng.*, *5575*, 16–30, doi:10.1117/12.572024.

Wielicki, B. A., and J. A. Coakley (1981), Cloud retrieval using infrared sounder data: Error analysis, *J. Appl. Meteorol.*, *20*, 157–169, doi:10.1175/1520-0450(1981)020<0157:CRUISD>2.0.CO;2.

Winker, D. M., W. H. Hunt, and C. A. Hostetler (2004), Status and performance of the CALIOP lidar, *Proc. SPIE Int. Soc. Opt. Eng.*, *5575*, 8–15.

Winker, D. M., W. H. Hunt, and M. J. McGill (2007), Initial performance assessment of CALIOP, *Geophys. Res. Lett.*, *34*, L19803, doi:10.1029/2007GL030135.

Wylie, D. P., and W. P. Menzel (1999), Eight years of high cloud statistics using HIRS, *J. Clim.*, *12*, 170–184.

Wylie, D., E. Eloranta, J. D. Spinhirne, and S. P. Palm (2007), A comparison of cloud cover statistics from the GLAS lidar with HIRS, *J. Clim.*, *20*, 4968–4981, doi:10.1175/JCLI4269.1.

Zhao, G., and L. D. Girolamo (2006), Cloud fraction errors for trade wind cumuli from EOS-Terra instruments, *Geophys. Res. Lett.*, *33*, L20802, doi:10.1029/2006GL027088.

S. A. Ackerman, B. Baum, S. Dutcher, R. Frey, R. E. Holz, and F. W. Nagle, Cooperative Institute for Meteorological Satellite Studies, University of Wisconsin-Madison, 1225 West Dayton Street, Madison, WI 53706, USA. (reholz@ssec.wisc.edu)

R. E. Kuehn and M. A. Vaughan, Science Systems and Applications, Inc., MS 475, Hampton, VA 23681, USA.